

# Modulations for Large Signal Constellations Coming from Embedding of Complete Graph

João de Deus Lima  
MCC-Uern/Ufersa, Mossoró, RN, Br.  
Email: jddeus@uol.com.br

Luana Priscilla R. C. de Lima  
UFERSA, Mossoró, RN, Br.  
Email: luana.lima@mcc.ufersa.edu.br

Wilken Charles Dantas de Melo  
MCC-Uern/Ufersa, Mossoró, RN, Br.  
Email: wilkencharles@gmail.com

**Abstract**—The integrated system of data transmission, encoding, modulation and block channels are projected in dependent ways with the purpose of getting an integrated action from those elements, and the elimination of additional devices with incompatibility treatment, caused by inadequate choice of some those components. In this system, the modulation and encoding projects take place in topological spaces  $(\Omega, d)$ , where  $\Omega$  is Riemannian manifolds and  $d$  is a metric on  $\Omega$ , which the discrete memoryless channel  $C_m$ , like a graph, is embedded. For each embedding  $C_m \hookrightarrow \Omega$ , it's possible to determine accurately a topological modulation project on  $\Omega$ , in the sense of knowing the decision regions (or Voronoi's regions) of each constellation signal. The paper's purpose is to identify topological projects of modulation on surfaces for large constellations, mainly the regular modulations. The procedures to obtain these projects are based on the method of the current graph developed by Gustin and Youngs and used in the proof of Color Graph Conjecture by Heawood.

## I. INTRODUCTION

In the model blocks of the integrated system (IS) shown in Fig. 1, the combination  $m$ -ary input in the modulator, the physical channel, and the  $n$ -ary output in the demodulator are modeled as a discrete memoryless channel (DMC), denoted by  $C_n$ . The modulation projects which come from partitions of 2-cells embedding of the complete graph  $K_n$  (associated to DMC [2]) in surface  $\Omega_i$ ,  $i = 1, 2, 3, 4$ .

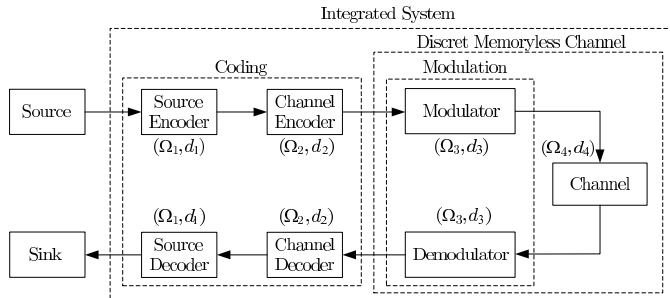


Fig. 1. Model blocks of integrated system

In IS, the metric spaces are considered the same. The objective of this approach is to obtain a system more efficient than an integrated system with a traditional data transmission, with the main blocks acting in a compatible

way, and providing a great number of options modulations for the same channel. Topological parameters of efficiency modulation are shown in Fig. 2. It's known that the efficiency of the modulation depends on the genus and regularity degree  $\alpha$  (number of regions of the same type), additionally, it is shown in [2] that they still depend on the number of edges of the regions and border components of the surface. The identification of these parameters is very important in order to know the IS performance.

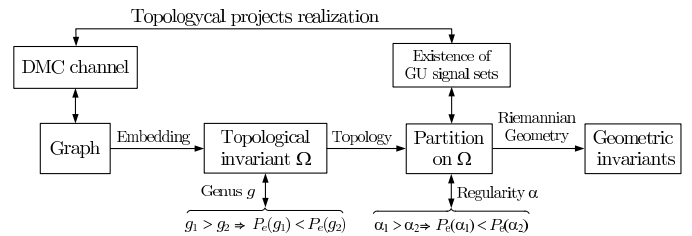


Fig. 2. Proposal overview (Adapted [3])

The identification process consists in mapping each region of the embedding and identifying the partition and surface. The regions are mapped through *orbital sequence* an orbital sequence which describes the order of the vertices belonging to the closed curve that defines the border of the region. The identification methods of oriented embedding in the complete graph  $K_n$  are presented for  $n$  values relatively high and regular models of embedding that get close to the maximum model of local regularity, according to the topological parameters of modulation efficiency related previously. Each embedding identified in this work is a topological project of modulation for a constellation with a large number of signals.

This work has the following structure: considerations about the method of the *current graph* current graph and examples of *Kirchhoff's Current Law*; the application of the current graph in the process of embedding identification of  $K_n$  followed by examples through a *gear system*, a method described in an algorithm form; a proposal of generating maximum and regular embeddings through disturbances in the rotation of  $K_n$ ; the results; and conclusions.

### A. Current Graph

The existence of current graph will be analyzed in the tetrahedron and triangular prism. It will be included in this session, some definitions and main relationships used in this work. A *graph* with  $p$ -vertices  $v_1, \dots, v_p$  and  $q$ -edges  $e_1, \dots, e_q$ , will be denoted by  $G(p, q)$ . The *incident arcs* to  $v_i \in G$  will be indicated by  $e_{i_1}, \dots, e_{i_h}$ , where  $h$  is the *degree* of vertex  $v_i$ , indicated by  $\circ(v_i) = h$ . If each edge of  $G$  contains an orientation (one arrow indicating the positive direction), then  $G(p, q)$  is called an *oriented graph*. The identification of the genus of an oriented surface for embedding graph is given by:

$$\chi(\Omega) = 2 - 2g \quad \text{if } \Omega \equiv gT \quad (1)$$

where  $gT$  represents the oriented surface of genus  $g$ .

The current graph consists of a group  $\Gamma$ , graph  $G$  drawing (not necessarily embedded) in the plane, and a label function  $\varphi$  that associates each direct edge of  $G$  to an element of  $\Gamma$ . The only requirement is that the inverse arcs are associated to the inverse elements of  $\Gamma$ .

We say that a Kirchhoff's Current Law (KCL) exists on  $G(p, q)$  if the sum of the currents in each vertex of  $G$  is equal to zero. The graph  $G$  with KCL and label with different non-null elements of the additive group  $\mathbb{Z}_{q+1} \setminus \{0\}$  is called *current graph*. In the current graph, current intensity assumes values in the set  $\Lambda = \{-q, -q+1, \dots, -2, -1, 1, 2, \dots, q-1, q\}$ , however, the KCL on  $G$  shows only positive values (the negative values are associated to opposed currents). More precisely, a current law on  $G$  should satisfy the conditions of the following linear system

$$\sum_{j=1}^{\circ(p_i)} \xi(e_{i_j}) e_{i_j} = 0, \quad \forall i \in \{1, 2, \dots, p\} \quad (2)$$

where  $\xi : \Lambda_{i_j} \rightarrow \{-1, 1\}$  is the function signal defined by:  $\xi(e_k) = 1$ , if the direction of the arrow points toward  $v_i$ , otherwise,  $\xi(e_k) = -1$ .

Particularly, the examples (1a) and (4a) in Fig. 3, show that it's possible to construct one KCL on a tetrahedron and triangular prism, since there is one solution of the system (2),  $S = (a_1, a_2, \dots, a_{2q})$ , composed by  $2q$ -tuple of different elements in  $\Lambda$ .

Fig. 3 (1b) contains the current graph corresponding to the rotation  $\sigma_1$  on tetrahedron; (1c) shows that the circuits are:  $\gamma_1 = (7, 12, 9)$ ,  $\gamma_2 = (11, 4, 3)$ ,  $\gamma_3 = (2, 5, 6)$ ,  $\gamma_4 = (8, 10, 1)$ ; therefore, a partition of the form  $4R_3$ ; of the Euler characteristic,  $\chi(\Omega) = 4 - 6 + 2 = 0$ , thus, by equality (1), the graph (1a) with the rotation  $\sigma_1$  is embedded in the sphere, i.e.,  $\Omega \equiv S$  (homeomorphic to the sphere). In the simplified form, this embedding is indicated by  $G(\sigma_1) \hookrightarrow S \equiv 4R_3$ . In a similar way, it was concluded that the other examples of embedding of the tetrahedron in (2) and (3) are respectively:  $G(\sigma_1) \hookrightarrow T \equiv R_3R_9$ . Only these three types of partitions were found coming from tetrahedron embedding.

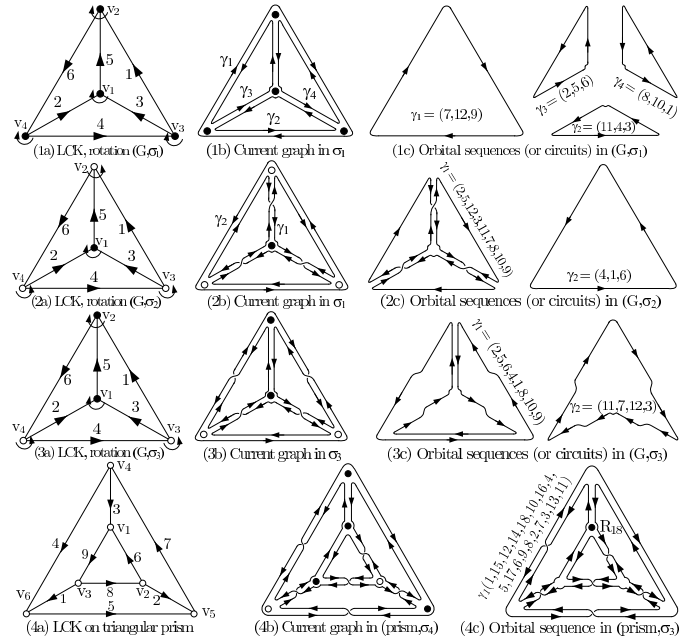


Fig. 3. Kirchhoff's Current Laws, current graphs and circuits on tetrahedron and triangular prism

The triangular prism embedding is given by  $G(\sigma) \hookrightarrow 2T \equiv R_{12}$ , an important example of a maximal circuit. It will be used to construct the minimal embedding of graph  $K_{19}$ .

1) *Current Graph and Identification Process*: The complete current graph method can be found in [4]. We include here only the main definitions.

A *rotation* of the vertex  $A$  of graph  $G$  is one oriented cyclic order (or one cyclic permutation) for all the incident arcs with  $A$ . A *rotation*  $(G, \sigma)$  is one rotation for each vertex of  $G$ .

Often, it is customary to represent a graph  $G$  with rotation in the plane in such a way that a clockwise (or counterclockwise) reading of the arcs incident with a vertex provides the rotation that vertex. Moreover, if the reading is to be clockwise (or counterclockwise) the vertex is represented by a small filled-in black (empty) circle such as  $\bullet$  ( $\circ$ ) [4]. In the following way, we can describe the rotation of a graph (see Fig. 3).

2) *Rotation Corresponding to a Minimal Embedding*: In this work, regular embedding is identified from disturbances in rotation corresponding to a minimal embedding. It's said that  $G \hookrightarrow gT$  is the *minimal embedding* of graph  $G$  in surface  $gT$ , if there is not an embedding of  $G$  in  $g'T$  such that  $g' < g$ . The rotation inducing exactly one only circuit that is called *circular rotation*, for instance, the rotation  $\sigma_4$  of the Fig. 3(4b).

Minimal embedding rotation of  $K_n$  is obtained from a circular rotation  $P_0$ , traveling once the  $2q$  arcs of one circular circuit of  $G(p, q)$ , starting at the arc 1, i.e.:

$$P_0 = (c_0 = 1, c_1, c_2, \dots, c_n), \quad (3)$$

where  $n = 2q$ . In this case,  $P_0$  is considered the permuta-

tion of the vertex 0 de  $K_n$ , and for every  $i = 1, 2, \dots, n-1$ , the permutation of the vertex  $i$  is considered the by adding  $i$  on each element of  $P_0$ :

$$P_i = P_0 + i = (c_0 + i, c_1 + i, c_2 + i, \dots, c_n + i). \quad (4)$$

If each circuit induced by a rotation  $\sigma$  for a graph has length three, then it is called a *triangular rotation*. A circuit of length three is sometimes called a *triangle*. Suppose that  $G$  has no vertices of valence  $\leq 1$ . Then, there are no circuits shorter than triangles. Therefore a *triangular rotation* of  $G$  is a *maximal rotation* [4]. A maximal rotation corresponds to a minimal embedding.

## II. IDENTIFICATION PROCESS FROM GEAR SYSTEMS

It is easy to construct the circuits of small graph embedding and identify it immediately as is shown Fig. 3. In the case of a large complex graph, the plane model is confused and the identification of circuits is very hard. These ones will be identified from a local rotation of vertices called *gear system*.

The following remark is important because it defines one partition above the surface on which the modulation project is well defined as *Hausdorff's space* (the union of all regions is equal the whole space and the intersection between two regions is always empty).

*Remark 1:* Let  $G(\sigma) \hookrightarrow \Omega \equiv \cup R_i$  be an embedding. If  $\sigma$  has equal orientations in all vertices of  $G$ , then  $\cup R_i$  is a Hausdorff's space on  $\Omega$ .

Note that the rotation  $\sigma_1$  on the tetrahedron of the Fig. 3 has: equal orientation in all vertices,  $\cup R_i = T$ , and  $R_i \cap R_j = \emptyset$ ; as a result, the torus with the partition  $\cup R_i$  is a Hausdorff's space. The fundamental step of the identifying process is the mapping of the regions. The partition and surface are obtained through Euler characteristic and equality (1). The region mapping depends only on the local behavior of rotating vertices. The embedding of interest is one that causes a partition of the type Hausdorff's space. Through the Remark 1 it must take the same orientation for all the vertices. Particularly, it will used in the clockwise orientation ( $\bullet$ ). The region's mapping will take place on a graphic scheme called *gear system*, as shown in Fig. 4.

### A. Identification Process $K_{13}$

The rotation of a vertex of  $K_{13}$  contains 12 elements, the same number of elements of  $\Gamma$  in the rotation  $(G, \sigma_1)$  of the Fig. 3(2b). As the tetrahedron doesn't have circular rotation, let us take the circuits  $\gamma_1$  and  $\gamma_2$  of the rotation  $(G, \sigma_1)$ , to compose the only circuit  $\gamma = \gamma_1 \gamma_2 = (2, 5, 12, 3, 11, 7, 8, 10, 9, 4, 1, 6)$  (operation known by *amalgamated product*) and to use it as  $P_0$  to obtain, through

formula (4), the rotation  $\sigma$  of  $K_{13}$ :

0.	2	5	12	3	11	7	8	10	9	4	1	6
1.	3	6	0	4	12	8	9	11	10	5	2	7
2.	4	7	1	5	0	9	10	12	11	6	3	8
3.	5	8	2	6	1	10	11	0	12	7	4	9
4.	6	9	3	7	2	11	12	1	0	8	5	10
5.	7	10	4	8	3	12	0	2	1	9	6	11
6.	8	11	5	9	4	0	1	3	2	10	7	12
7.	9	12	6	10	5	1	2	4	3	11	8	0
8.	10	0	7	11	6	2	3	5	4	12	9	1
9.	11	1	8	12	7	3	4	6	5	0	10	2
10.	12	2	9	0	8	4	5	7	6	1	11	3
11.	0	3	10	1	9	5	6	8	7	2	12	4
12.	1	4	11	2	10	6	7	9	8	3	0	5

The gear system corresponding to the rotation  $\sigma$  is shown in the Fig. 4. In this one, the integer  $i \in \Gamma$ , in the middle of central circle, indicates the index of the vertex  $v_i$  of  $K_{13}$ ;  $j \in \Gamma$  on a arrow next to the circumference, indicates the index of the vertex  $v_j$  adjacent to the edge  $(v_i, v_j)$  in the rotation of  $v_i$ ; and the pair  $k, s$  defines the  $s^{th}$  element of the  $k^{th}$  orbital sequence.

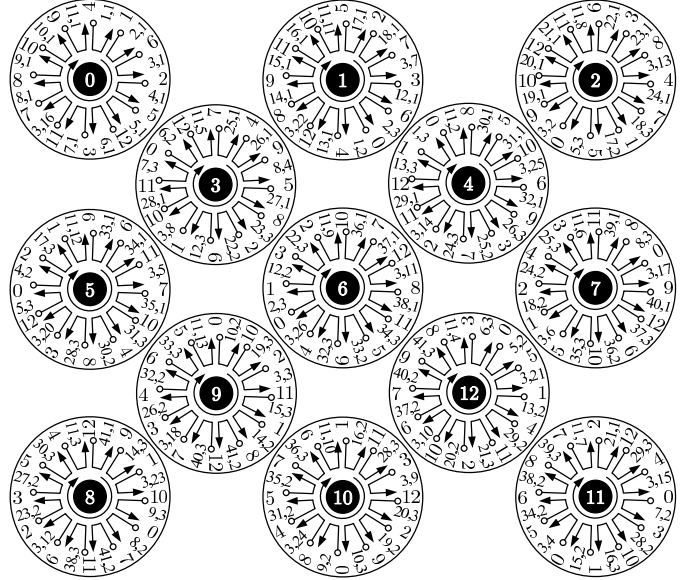


Fig. 4. Gear system of rotation  $(K_{13}, \sigma)$

It is concluded that the gear system, the embedding of the graph  $G \hookrightarrow \Omega$  is identified through the following:

*Algorithm 1:* If  $E(\sigma)$  is the gear system of rotation  $(G(p, q), \sigma)$ , then the  $i^{th}$  orbital sequence of the embedding  $G \hookrightarrow \Omega$  is given through the following steps:

- 1) Choose an adjacent vertex  $v_{j_1}$  in rotation of  $v_i$  and write down, between the consecutive adjacent vertices  $v_{j_1}, v_{j_1+1}$  of  $v_i$ , the pair  $i, 1$ .
- 2) Find the adjacent vertex  $v_{j_2}$  of  $v_{j_1+1}$  equal to  $v_i$ , and write the pair  $i, 2$  between the consecutive adjacent vertices  $v_{j_2}, v_{j_2+1}$  of  $v_{j_1+1}$ .
- 3) In the  $m^{th}$  step, find the adjacent vertex  $v_{j_m}$  of  $v_{j_{m-1}+1}$  equal to  $v_{j_{m-2}+1}$ , and write the pair  $i, k$  between the consecutive adjacent vertices  $v_{j_m}, v_{j_m+1}$ .

de  $v_{j_{m-1}+1}$ .

- 4) Continuing the constructing process, write the sequence  $\tau$  of length  $d_1 + 2$ , such that the last two terms are the same as the first one, i.e.:

$$\tau = (i, j_1 + 1, j_2 + 1, j_3 + 1, \dots, j_{d_1-1}, i, j_1 + 1). \quad (5)$$

In this case, the orbital sequence  $\gamma_1 = (i, j_1 + 1, j_2 + 1, j_3 + 1, \dots, j_{d_1-1})$  defines the frontier of a region of  $d_1$ -edges,  $R_{d_1}$ , of the oriented embedding  $G(\sigma) \hookrightarrow \Omega$ .

- 5) Choose an adjacent vertex  $v_t$  of  $v_u$  in such a way that  $(t, u)$  is not a sub-sequence of  $\gamma_1$ , and repeat steps 1) through 4) to obtain the orbital sequence  $\gamma_2$  of length  $d_2$ . The process finishes when  $\sum_i^k d_i = 2q$ , and the embedding  $G(\sigma) \hookrightarrow \Omega \equiv R_{d_1} R_{d_2} \dots R_{d_k}$  is obtained.

All the embeddings of this work are identified through Algorithm 1 and the gear system. For example, the orbital sequences of rotation  $(K_{13}, \sigma)$  are given by:

1(0,1,4), 3(0,2,9,11,5,7,1,3,10,12,6,8,2,4,11,7,9,3,5,12,1,8,10,4,6),  
 2(0,6,1), 4(0,5,2), 5(0,12,5), 6(0,3,12), 11(0,4,8,12,3,7,11,2,6,10,1,5,9),  
 7(0,11,3), 8(0,8,7), 9(0,10,8), 10(0,9,10), 12(1,6,3), 13(1,12,4), 14(1,9,8),  
 15(1,11,9), 16(1,10,11), 17(1,2,5), 18(1,7,2), 19(2,10,9), 20(3,9,4),  
 21(2,12,10), 22(2,11,12), 23(2,3,6), 24(2,8,3), 25(2,7,4), 26(3,4,7),  
 27(3,8,5), 28(3,11,10), 29(4,12,11), 30(4,5,8), 31(4,10,5), 32(4,9,6),  
 33(5,6,9), 34(5,11,6), 35(5,10,7), 36(6,7,10).

Note that, rotation of  $(K_{13}, \sigma)$  circuits is composed by 42 regions: 39 triangular, one of 13 and the other of 26 edges, this way, an embedding of the form  $K_{13}(\sigma) \hookrightarrow 13T \equiv 39R_3R_{13}R_{26}$ . It is an embedding close to minimal and can be used for a project of modulation on the surface  $13T$ , for a constellation of 41 signals, or on the surface with two border's components  $13T_2$ , for a constellation of 39 signals of the type *geometrically uniform*.

The procedures above show that the rotations of the tetrahedron  $\sigma_1$  and  $\sigma_3$  generate the embedding described in Table I. As  $\sigma_3$  possesses the maximum circuit of the tetrahedron, observe that it is on the surface of smaller genus among generators circuits as shown before in Fig. 3.

TABLE I

THIS EMBEDDING COMES FROM TETRAHEDRON ROTATIONS  $\sigma_1$  AND  $\sigma_3$

Rotation $P_0$	Irregular	Regular
$\sigma_1$ (7,12,9,11,4,3,2,5,6,8,10,1)	$26T \equiv 14R_3R_{104}$	$26T_1 \equiv 14R_3$
$\sigma_3$ (2,5,6,4,1,8,10,9,11,7,12,3)	$19T \equiv 26R_313R_6$	$19T_{13} \equiv 26R_3$

1) *Minimal Embedding of  $K_{19}$* : The vertex's rotation of  $K_{19}$  has 18 adjacent vertices, a number equal to twice the number of edges on the triangular prism  $\Pi_3$ . Using (4) to construct the rotation  $(K_{19}, \varrho)$  from circular rotation in Fig. 3(4c),  $P_0 = (1, 15, 12, 14, 18, 10, 16, 4, 5, 17, 6, 9, 8, 2, 7, 3, 13, 11)$ , we obtain a minimal embedding  $K_{19}(\sigma') \hookrightarrow 20T \equiv 114R_3$  (identified through Algorithm 1). This is a unusual example of triangular circuit and regular modulation for a

constellation of 113 signals of the geometrically uniform type on 20-tory.

### III. ROTATION DISTURBANCE OF $K_n$

The aim is to investigate the effect of few alterations in the rotation of a minimum embedding of  $K_n$  to obtain a regular modulation.

*Definition 1*: A *disturbance* of a  $(K_n, \sigma)$  rotation is any permutation of the vertex's rotations of  $K_n$ . Two particular cases will be considered disturbances of the vertex  $j$  of  $K_n$ :

- d1: permutation of two isolated adjacent vertices:

$$j(\dots a_{ih} \dots a_{ik} \dots) \rightarrow j(\dots a_{ik} \dots a_{ih} \dots);$$

- d2: permutation of  $k$  consecutive pairs of vertices:

$$j(\dots a_{ih}a_{i,h+1}a_{i,h+2}a_{i,h+3} \dots a_{i,h+k-1}a_{i,h+k} \dots) \rightarrow j(\dots a_{i,h+1}a_{ih}a_{i,h+3}a_{i,h+2} \dots a_{i,h+k}a_{i,h+k-1} \dots).$$

Concerning to the rotation's disturbances the following results were enunciated and demonstrated in [2].

*Proposition 1*: Let  $(K_n, \sigma)$  be a minimal oriented embedding of complete graph  $K_n$ , then:

- 1) d1 produces two hexagonal orbits:  $\gamma_1 = (j, a_{ik}, a_{i,h+1}, j, a_{ih}, a_{i,h-1})$  and  $\gamma_2 = (j, a_{i,k-1}, a_{ih}, j, a_{i,k+1}, a_{ik})$ ;
- 2) d2 produces an orbit with  $3 + 6k$  arcs:  $R_{3+6k} = (j, a_{i,h+1}, a_{ih}, j, a_{i,h+3}, \dots, a_{i,h+k}, a_{i,h+k-1}, j, a_{i,h+k+1}, a_{i,h+k-3}, a_{i,h+k}, j, \dots, j, a_{ih}, a_{i,h+3}, j, a_{i,h-1})$ .

*Theorem 1*: Let  $R_s, R_t, R_u, R_v$  be the different neighboring regions, the vertices  $a_{ih}, a_{ik}$  not consecutive but adjacent to vertex  $j$  of  $K_n$ . Then disturbance d1 produces two regions  $R'_{i+u}$  and  $R''_{j+v}$  with  $i + u$  e  $j + v$  edges, respectively.

*Theorem 2*: The disturbance d2 transforms the  $2k + 1$  affected regions  $R_{s_1}, R_{s_2}, \dots, R_{s_{2k+1}}$  in only one region with a number of edges equal to  $\sum_{i=1}^{2k+1} s_i$ .

#### A. Regular Modulations Via Disturbances

Proposition 1 will be applied at the minimal embedding  $K_{13} \hookrightarrow 8T \equiv 51R_3 + R_6$  to generate regular modulation with regions of  $3k$  edges.

*Proposition 2*: [2] If d1, d2 are properly combined, then maximal partition  $(K_{13}, \sigma)$  (minimal embedding) produces regions of  $3k$  edges.

The purpose of Proposition 2 is to obtain regular modulation models as those related in Table II.

In Table II, the column  $\Omega_r$  indicates the surfaces with borders where they are the respective regular modulations related in the column G.U. (geometrically uniform). Observe that  $29T$  has maximum genus,  $50R_3$  shows the largest number of signals (regions),  $5R_{24}$  has the regions with the largest number of edges, and  $6R_3$  is in the surface with the largest number of border components  $19T_{23}$ . These are the models that maximize the topological elements that make influence the modulation performance.

TABLE II  
REGULAR EMBEDDING OF  $K_{13}$  WITH REGIONS  $R_{3k}$ ,  $k = 1, 2, \dots, 8$

Borderless surface		Surface with board	
$\Omega$	Irregular	$\Omega_r$	G.U.
$8T$	$50R_3R_6$	$8T_1$	$50R_3$
$22T$	$17R_62R_32R_92R_{15}$	$23T_6, 23T_{21}$	$17R_6, 2R_3, 2R_9, 2R_{15}$
$19T$	$23R_66R_3$	$19T_6, 19T_{23}$	$23R_6, 6R_3$
$23T$	$13R_95R_32R_6R_{12}$	$19T_8, 19T_{16}, 19T_{19}$	$13R_9, 5R_3, 2R_6$
$23T$	$15R_95R_3R_6$	$23T_6, 23T_{16}$	$15R_9, 5R_3$
$24T$	$15R_9R_{12}3R_3$	$24T_4, 24T_{16}$	$15R_9, 3R_3$
$24T$	$11R_{12}8R_3$	$24T_8, 24T_{11}$	$11R_{12}, 8R_3$
$26T$	$9R_{15}5R_3R_6$	$26T_6, 26T_{10}$	$9R_{15}, 5R_3$
$28T$	$7R_{18}R_{21}3R_3$	$28T_4, 28T_8$	$7R_{18}, 3R_3$
$28T$	$6R_{21}R_{10}R_{11}3R_3$	$28T_5, 28T_8$	$6R_{21}, 3R_3$
$29T$	$5R_{24}R_{22}R_82R_3$	$29T_4, 29T_7$	$5R_{24}, 2R_3$

### B. Regular Modulations From $K_{19}$ Embedding

The minimal embedding of  $(K_{19}, \varrho)$  in Subsection II-A1 was constructed from an unedited circular rotation of the triangular prism in Fig. 3(4b). It is an example of a triangular rotation that has the property of generating modulations with a high degree of regularity. Although, it takes more time to identify the embedding of  $K_{19}$ , the difficulty of manipulating the Algorithm 1 is the same for each graph. Due to time constraints only the three examples of embedding were identified in Table III, however, any rotation of  $K_{19}$  can be identified through Algorithm 1.

TABLE III  
REGULAR MODULATION OF  $K_{19}$  WITH REGIONS  $R_{3k}$ ,  $k = 1, 2, 3$

Maximum regularity	Borderless surface		Surface with border	
	$\Omega$	Partition	$\Omega_r$	G.U.
$114R_3 \leftrightarrow 20T$	$20T$	$114R_3$ (G.U.)	—	—
$56R_62R_3 \leftrightarrow 48T$	$46T$	$52R_610R_3$	$46T_{10}, 46T_{52}$	$52R_{10}, 10R_3$
$38R_9 \leftrightarrow 58T$	$56T$	$34R_94R_64R_3$	$56T_8, 56T_{38}$	$34R_9, 4R_6, 4R_3$

In the first column of Table III we include, for comparison effect, the maximum regularity model of each case. Note that the only minimal embedding related in Table III reached the maximum regularity model. The other two embedding differ in their respective models of maximum regularities only in 2 units of genus and of 4 regions with the largest number of regularities. These embedding examples represent the regular modulations identified in this work with the largest number of signals: in the borderless surface  $20T$  with 114 signals and Vorony's triangular regions; in the surface with borders  $46T$  with 56 signals and Vorony's hexagonal regions; and in the surface with borders  $56T$  with 34 signals and Vorony's regions of 9 edges. We remember that these examples were constructed with a minimal effort, using Proposition 2, gear system and Algorithm 1.

### IV. CONCLUSION

The purpose of this work is the development identification methods of oriented embedding of the complete graph

$K_n$ , for  $n$  values relatively large, according to efficient topological parameters of modulation given by relations of overview proposal (see Fig. 2).

The current graph method used in the identification process shows that it is very efficient. In spite of the calculations and constructions of the identification process having been done manually (no programming routines), results were obtained from regular embedding of complete graph in cases which the complexity is very high. The application of Algorithm 1 in the identification of topological projects modulation practically has no limits. It can be used comfortably in the gear system of any kind of a graph, independent of the amount of vertices.

Regarding the method of the vertices disturbances, its efficiency was confirmed in the production of maximal embedding through permutations of columns, and it was shown in Proposition 2 that it is possible to combine the two types of disturbances d1 and d2, appropriately, in a maximal rotation of the graph, to produce regular modulations with regions of  $3k$ -sides,  $k = 1, 2, 3, \dots$ . The method of the disturbances can be used to produce other types of topological projects of regular modulations, and it is not only applied to maximal rotations, but other types can be used, besides the minimal one.

The results of this work provide precise answers according to the form and existence of topological projects of modulations, a fundamental stage of the project in an integrated system of data transmission. This is the information which validates and rewards the effort on the part of the planner, in the search and elaboration of more efficient modulation projects in the field of the Riemannian manifolds.

### V. ACKNOWLEDGMENT

The authors would like to thank to FAPERN and CNPq for their financial support, and also to formally acknowledge anonymous referees for their insightful comments, suggestions, and criticism, which considerably improved the quality for the presentation of this paper, and Bradley Ray Stewart for translation assistance and review.

### REFERENCES

- [1] J. D. Lima e R. Palazzo Jr., *Identification and Algebraic Structure of Compact Surfaces with and without Borders Derived from Embedding of Discrete Memoryless Channels*, Doctoral Dissertation, School of Electrical and Computer Engineering, State University of Campinas, Brazil, 2002, (in Portuguese).
- [2] L. P. R. C. Lima e J. D. Lima, *Modulation's Project on Topological Surface Associated to the Discrete Memoryless Channels: a solution for a Integrated System*, Master Dissertaton, Computer Science Mester UERN/UFERSA, 2009. (in Portuguese).
- [3] R. G. Cavalcante, H. Lazari, J. D. Lima and R. Palazzo Jr., A new approach to the design of digital communication systems, *DIMACS Series in Discret Mathematics and Theoretical Computer Science*, 68 (2005) 145-177.
- [4] G. Ringel, *Map Color Theorem*, New York, Springer-Verlag, 1974.
- [5] S. Stahl, The Embeddings in a Graph - A Survey, em "Journal of Graph Theory", 2 (1978) 275-298.
- [6] J. W. T. Youngs and F. Ciryl, Minimal imbeddings and the genus of a graph, *J. Math. Mech.*, 12 (1963) 303-316.